Experimental and Theoretical Study of the Equation of State of Liquid Ethylene

Jorge C. G. Calado,† Paulette Clancy,* Andreas Heintz, and William B. Streett

School of Chemical Engineering, Cornell University, Ithaca, New York 14853

A gas-expansion method has been used to measure the density of liquid ethylene at 19 temperatures between 110 and 280 K and at pressures up to 1300 bar. The results have been fitted to an equation of state that has been used to calculate the following properties of the compressed liquid: density, isothermal compressibility, thermal expansivity, thermal pressure coefficient, configurational internal energy, and entropy relative to the entropy of the ideal gas at the same density and temperature. The following properties of the saturated liquid have been calculated: enthalpy of vaporization, configurational internal energy, isothermal compressibility, thermal expansivity, and thermal pressure coefficient. The densities and mechanical coefficients were also estimated for the liquid along the melting line. The density, internal energy, and entropy results have been interpreted in the light of a perturbation theory using several intermolecular potential models for ethylene.

Introduction

The importance of ethylene in industrial processes has caused an increasing interest in accurate measurements and calculations of its thermodynamic properties. After a critical compilation of data up to 1972, published by the IUPAC commission (*1*), the works of Douslin and Harrison (*2*) and Hastings et al. (*3*) have concentrated on *PVT* measurements in the critical and supercritical region. An equation of state based on the *PVT* data available up to 1975 has been published by Bender (*4*). The work of Straty (*5*) has provided *PVT* data in the fluid region at higher pressures, including several points on the melting curve. Furthermore, a new comprehensive data compilation, coordinated by NBS, is in progress (*6*). There still remains a lack of *PVT* data at pressures above 350 bar over a range of temperature from the triple point to the critical temperature. In this work we present 800 *PVT* measurements, covering a range of 110–280 K in temperature and pressures up to 1300 bar. The data have been fitted to the Strobridge equation of state, from which thermodynamic properties such as compressibility, thermal expansion coefficient, configurational internal energy, and entropy have been calculated.

Besides its technical significance ethylene belongs to the class of relatively simple molecules that are of special interest for application of modern molecular perturbation theories. Vapor pressure, density of the saturated liquid, and some *PVT* data in the supercritical region have already been successfully described by perturbation theory, using the known quadrupole moments for the orientation-dependent part of the perturbation potential and a suitable Lennard-Jones n–6 potential for the reference fluid (*7*, *8*). In the theoretical section of this work we extend these calculations of the perturbation theory to state conditions covered by our experimental *PVT* points, to test the applicability of the theory in the high-pressure region of liquid ethylene. Comparison of these results with those obtained by using other potential models for ethylene have also been made.

† Permanent address: Complexo I, Instituto Superior Tecnico, 1096 Lisboa, Portugal.

Experimental Section

The apparatus used in this work, based on an expansion principle, is a modification of the apparatus described by Streett and Staveley (*9*). A schematic diagram is shown in Figure 1. The cell is first filled with liquid ethylene, which is then compressed to a pressure of about 1200 bar. Liquid ethylene at high pressure is expanded from the pressure cell, held at fixed temperature in the cryostat, into the calibrated expansion volume at 303.15 K, where the final pressure is 1.5 bar or less. The mass of fluid in the expansion volume is calculated from the virial equation, truncated after the second term; after corrections for redundant volume and other effects, this yields the density in the pressure cell before expansion.

In previous experiments with an apparatus of this type (*9*–*11*) a cell with an internal volume of 3.6 cm^3 was used, and a complete expansion was made for each *PVT* point (see ref *9* for details). In this work, a cell of volume 27.5 cm^3 has been used and expansions have been made by a differential method, that is, by expanding from the highest pressure ($\simeq$1200 bar) through pressure steps 10–50 bar and measuring the amount of fluid expanded at each step. When a pressure slightly higher than the saturation vapor pressure is reached, the remaining contents are expanded to obtain the absolute density at that pressure. Since it is necessary to measure the high pressure at each step, the expansions are made through valve E from a volume that includes not only the cell but also a "redundant volume" consisting of the differential pressure indicator (DPI) and the valves and tubing between the pressure cell, the DPI, and valve E. (The DPI is a diaphragm device used to separate ethylene in the expansion system from oil in the dead-weight gauge.) During these expansions valves B and D remain closed. The results of these expansions give the mass of fluid in the combined volume (the pressure cell plus the redundant volume) as a function of pressure. Separate expansions are then made from the dummy line (valve A closed and B open), over the same pressure range. The volume of the dummy line, connected to valve B, is equal to that of the line connecting the pressure cell to valve A. These expansions give the mass of fluid in the redundant volume, as a function of pressure; subtracting this mass from that obtained in the expansions from the cell gives the mass (and hence the density) of the fluid in the cell as a function of pressure. A complete isotherm, typically 30–50 data points, is obtained in a single run over a period of 5–6 h. Following each run, the ethylene is recycled by condensing it into the stainless-steel cylinder immersed in liquid N_2. When this cylinder is warmed to room temperature, the pressure rises to about 50 bar, and this is used as input to the diaphragm compressor to compress the ethylene into the cell for the next experiment.

Temperatures in the cryostat are controlled to within ±0.03 K by maintaining a constant pressure in a pure liquid boiling under its own vapor pressure (*9*) (CH_4, CF_4, C_2H_6, CO_2, and CHF_2Cl were used in this work). Temperatures are measured by an NBS-calibrated platinum resistance thermometer and Mueller bridge, with an accuracy of ±0.01 K. High pressures are measured by a Ruska Model 2450 dead-weight gauge, with an absolute accuracy of 0.1% or better, and a precision of about 0.01%. Temperatures in the water bath are controlled

0021-9568/82/1727-0376$01.25/0

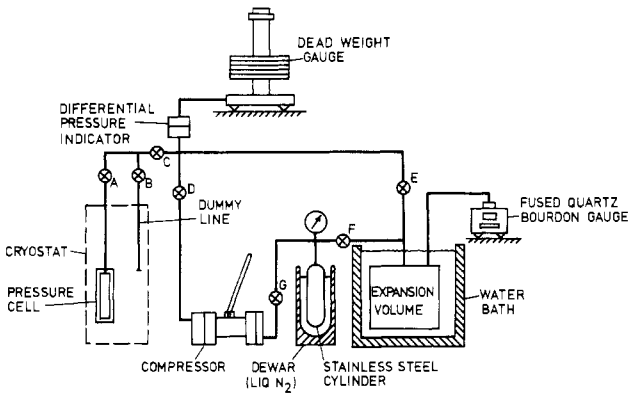

Figure 1. Experimental apparatus (see text for description).

to within ±0.01 K by an electronic temperature controller and measured by an NBS-calibrated mercury thermometer. Lower pressures in the expansion volume are measured by a Texas Instruments Model 142 fused quartz Bourdon gauge, with an absolute accuracy of about 0.015% and a precision of a few parts in 10^5.

Several corrections must be made to the raw data to obtain the desired results, the most important of these being the change in volume of the cell with pressure and the mass of fluid contained in the connecting lines and pressure gauge at the low pressure end. In practice most of the valves and tubing comprising the expansion system are located in the water bath to maintain their temperature constancy. The DPI and several segments of tubing between the cryostat and water bath are maintained at constant temperature by water circulated from the bath.

When this apparatus is used, the principal uncertainty in the final results is due to imprecise knowledge of the volumes of the system, mainly the pressure cell and the expansion volume. The expansion volume (≃3.5 dm^3 at atmospheric pressure) was measured by weighing with water and is known to within 0.02%. The final calibration of the cell volume has been made by requiring agreement between our results for ethylene at saturation and those of Haynes (*12*) and Menes et al. (*13*) which, although obtained by different methods, agree to within 0.05%. Saturation densities are obtained from our results by a short extrapolation from the lowest expansion pressure to the saturation vapor pressure. Assuming that the measurements of Haynes are correct, we estimate that the average absolute error in our measurements is about 0.1% in density.

The ethylene used in this work was C.P. grade from Liquid Carbonic. It was purified by double fractionation in a low-temperature distillation column with a reflux ratio of 19/20. The final purity is estimated to be better than 99.99%.

Results

The 800 *PVT* points have been measured by the method described above in the temperature range from 110 to 280 K and at pressures from the saturation pressure up to about 1300 bar. The data are recorded in Table I. For describing and interpolating these data the Strobridge equation of state has been used in the following form:

$$P = RT\rho + (A_1RT + A_2 + A_3/T + A_4/T^2 + A_5/T^4)\rho^2 + (A_6RT + A_7)\rho^3 + A_8T\rho^4 + (A_9/T^2 + A_{10}/T^3 + A_{11}/T^4)\exp[A_{18}\rho^2]\rho^3 + (A_{12}/T^2 + A_{13}/T^3 + A_{14}/T^4)\exp[A_{16}\rho^2]\rho^5 + A_{15}\rho^6 \quad (1)$$

With the exception of A_{18} this equation is linear in the coefficients A_i. These coefficients have been fitted to the experimental points by means of a weighted least-squares technique, described by Hust and McCarty (*14*). The quality of the fit is

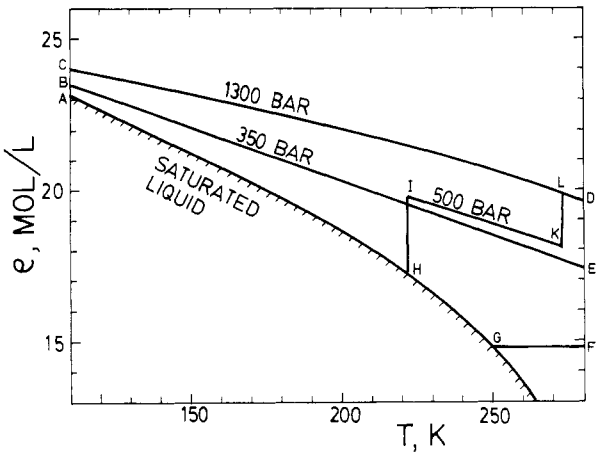

Figure 2. Density-temperature region covered by this work is the area ACDFG. The measurements of Straty (*5*) cover the region ABEFG, and the IUPAC compilation (*1*) covers the region HIKLDFG.

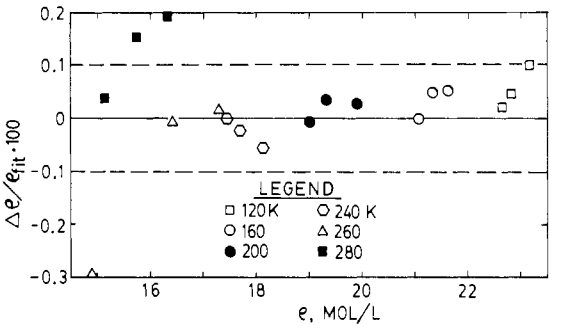

Figure 3. Relative deviations in density of the data of Straty (*5*) from eq 1 of this work. The dashed lines represent one standard deviation in the fitted data.

rather insensitive to the choice of the nonlinear constant A_{16}, and an appropriate value of A_{16} has been chosen, similar to that used in previous work on krypton and xenon (*10*, *11*). The coefficients A_1 to A_{16} obtained from the fitting procedure are given in Table II. Using these values eq 1 is valid only in the *PVT* range covered by the experimental data of this work. No further constraints have been imposed on eq 1; in particular the critical point is not represented. In general, application of eq 1 using A_i from Table II is not recommended in regions where the density is lower than 14.8 mol dm^{-3}.

One measure of the effectiveness of eq 1 in representing the experimental results is the magnitude of the difference $\Delta\rho$ between the experimental and calculated densities. For the 800 data points in Table I, the maximum value of $\Delta\rho$ is 0.35% and the average is about 0.1%. As the absolute accuracy of the experimental densities is estimated to be 0.1%, eq 1 represents the data within the experimental error. Comparison has been made with high-pressure density data reported by other authors. As shown in Figure 2 the *PVT* range covered by the measurements of Straty (*5*) lies within the range of our data, and in the region above 250 K and pressures up to 500 bar our data overlap with an equation of state reported by the IUPAC commission (*1*) and by the NBS study (*6*). As noted above, the saturated-liquid densities of Haynes (*12*) were used to calibrate our apparatus; hence, there is a forced agreement between those results and the saturated-liquid densities obtained by extrapolating our experimental isotherms to the saturation curve. Figures 3 and 4 show the comparison of the present data with those of Straty and the IUPAC equation for a series of representative points in the overlap regions. The results of McCarty and Jacobsen (*6*) were unfortunately not available for comparison when this study was made. With the exception of points near the critical temperature, the differences are within

Table I. Experimental Results of Density ρ at Pressure P and Temperature T

P/bar	ρ/ (mol L^{-1})	P/bar	ρ/ (mol L^{-1})	P/bar	ρ/ (mol L^{-1})
		T = 110.0 K			
400.09	23.736	141.79	23.350	52.07	23.173
358.97	23.672	127.60	23.326	37.03	23.153
307.44	23.632	115.75	23.305	23.73	23.114
286.36	23.556	106.32	23.287	15.97	23.099
254.75	23.508	92.65	23.260	11.13	23.093
226.08	23.467	84.26	23.243	7.94	23.089
200.52	23.430	77.07	23.228	6.45	23.087
164.22	23.385	70.36	23.213	5.29	23.085
158.46	23.376	63.15	23.197	0.00	23.081
		T = 120.0 K			
1003.16	24.155	342.89	23.236	78.13	22.739
930.82	24.065	307.79	23.176	71.35	22.726
861.23	23.976	275.60	23.116	66.36	22.717
795.99	23.888	245.57	23.063	53.38	22.694
733.72	23.802	218.66	23.017	34.76	22.588
673.54	23.719	194.69	22.978	17.88	22.669
617.68	23.639	173.64	22.935	13.72	22.669
563.90	23.563	154.90	22.896	11.73	22.635
513.62	23.491	139.01	22.863	10.10	22.619
466.36	23.424	125.26	22.834	7.89	22.604
422.06	23.359	104.39	22.791	5.80	22.603
381.08	23.296	86.83	22.756	0.01	22.625
		T = 130.0 K			
1076.34	23.962	338.35	22.863	92.77	22.390
1006.06	23.871	305.72	22.802	83.41	22.369
937.02	23.779	275.67	22.740	73.97	22.348
871.70	23.688	247.63	22.684	69.08	22.337
809.97	23.598	222.03	22.634	64.73	22.328
749.20	23.513	199.07	22.592	58.13	22.312
693.67	23.429	178.06	22.557	42.13	22.274
639.48	23.349	159.75	22.525	26.09	22.223
589.09	23.271	143.65	22.493	16.73	22.199
540.87	23.197	129.92	22.466	10.32	22.185
495.22	23.125	118.16	22.442	7.96	22.180
452.49	23.056	107.53	22.421	5.76	22.175
412.63	22.989	99.36	22.404	0.04	22.162
374.19	22.926				
		T = 140.0 K			
1126.33	23.666	353.57	22.459	76.82	21.868
1058.39	23.575	321.25	22.395	73.09	21.860
989.28	23.485	291.58	22.332	69.21	21.851
925.49	23.392	264.01	22.273	60.72	21.831
864.63	23.300	238.62	22.221	50.41	21.807
804.55	23.211	215.46	22.174	36.67	21.779
748.68	23.124	194.65	22.133	27.30	21.750
694.39	23.039	175.78	22.096	17.96	21.730
643.03	22.956	159.15	22.054	11.68	21.716
594.30	22.877	144.49	22.021	8.90	21.711
548.28	22.801	131.49	21.992	7.66	21.709
504.63	22.728	111.38	21.947	5.76	21.706
463.14	22.657	97.68	21.916	5.36	21.705
424.31	22.589	88.58	21.895	0.12	21.691
387.65	22.523	82.55	21.881		
		T = 150.0 K			
1096.85	23.287	390.69	22.121	66.94	21.359
1028.56	23.198	326.15	21.990	51.59	21.322
964.55	23.105	270.98	21.860	39.64	21.303
902.57	23.011	223.40	21.752	31.26	21.279
844.42	22.920	184.05	21.665	24.58	21.260
788.41	22.830	152.25	21.576	17.65	21.239
734.78	22.741	126.47	21.509	13.97	21.229
683.87	22.655	107.90	21.462	9.29	21.219
636.09	22.570	95.16	21.430	5.91	21.212
544.44	22.410	83.56	21.400	0.27	21.210
463.43	22.261	75.83	21.381		
		T = 160.0 K			
1123.09	23.014	353.74	21.652	77.50	20.930
1056.39	22.918	296.63	21.513	73.47	20.919
992.31	22.822	246.81	21.382	69.90	20.909
931.03	22.726	204.31	21.277	66.18	20.898
873.09	22.630	168.86	21.187	60.65	20.882
816.87	22.537	140.40	21.108	48.46	20.848
763.82	22.446	118.07	21.045	28.50	20.791
664.06	22.268	102.53	21.001	12.54	20.730
573.83	22.101	91.05	20.969	3.51	20.720
492.68	21.943	83.84	20.948	0.56	20.719
419.36	21.793				
		T = 170.0 K			
1129.01	22.727	271.46	21.039	56.08	20.405
1064.24	22.631	227.27	20.929	48.71	20.380
1001.95	22.534	189.29	20.828	41.32	20.355
943.11	22.436	157.84	20.730	32.27	20.324
886.61	22.339	132.67	20.653	25.61	20.297
832.64	22.243	113.11	20.592	18.01	20.269
781.47	22.149	99.17	20.547	13.42	20.254
684.86	21.964	89.43	20.516	10.76	20.246
595.71	21.791	80.53	20.487	8.12	20.239
515.96	21.626	75.55	20.470	6.17	20.233
444.31	21.469	71.31	20.456	5.29	20.229
380.67	21.320	67.42	20.443	1.05	20.214
321.95	21.179	62.16	20.426		
		T = 180.0 K			
1103.77	22.404	312.58	20.761	60.91	19.934
1045.19	22.306	265.27	20.617	55.72	19.914
984.85	22.210	224.32	20.492	48.38	19.885
928.98	22.113	189.08	20.388	39.62	19.852
876.32	22.015	159.49	20.290	28.77	19.805
825.47	21.918	135.26	20.207	19.71	19.769
776.65	21.824	115.60	20.138	14.62	19.749
729.15	21.730	95.66	20.065	11.90	19.739
684.86	21.638	84.25	20.023	9.77	19.733
642.30	21.549	77.76	19.998	7.38	19.723
562.37	21.376	73.73	19.983	5.53	19.713
496.92	21.204	70.84	19.972	5.19	19.711
424.68	21.055	67.77	19.960	1.82	19.694
365.58	21.905	64.86	19.949		
		T = 190.0 K			
1119.89	22.127	427.37	20.676	69.38	19.464
1060.59	22.033	371.64	20.523	60.64	19.425
1004.13	21.936	321.88	20.375	47.82	19.368
950.39	21.838	276.56	20.229	38.72	19.334
898.98	21.740	237.05	20.098	28.71	19.279
849.81	21.643	202.31	19.981	18.17	19.223
801.91	21.547	172.33	19.875	12.85	19.202
756.64	21.452	136.05	19.738	10.05	19.194
713.68	21.357	110.18	19.635	7.94	19.185
631.76	21.176	93.16	19.565	5.60	19.170
557.82	21.007	80.55	19.512	2.96	19.155
489.83	20.835				
		T = 200.0 K			
1150.25	21.911	401.21	20.232	110.37	19.170
1093.61	21.811	375.14	20.154	98.57	19.115
1037.45	21.710	350.53	20.077	89.74	19.072
983.80	21.609	326.99	19.999	83.61	19.042
932.77	21.508	304.95	19.922	77.62	19.012
882.82	21.409	283.88	19.848	73.82	18.993
835.12	21.309	264.50	19.777	66.99	18.958
789.65	21.210	245.49	19.710	60.83	18.925
746.01	21.112	227.93	19.646	47.88	18.855
703.81	21.016	211.49	19.586	32.74	18.775
663.34	20.922	196.22	19.529	26.01	18.730
624.90	20.828	181.85	19.475	21.44	18.701
587.72	20.737	168.76	19.421	15.45	18.661
551.54	20.645	156.57	19.371	11.31	18.644
518.36	20.560	145.59	19.325	9.18	18.630
487.10	20.476	135.17	19.281	7.36	18.615
456.93	20.393	125.73	19.239	5.28	18.597
428.53	20.312	117.59	19.203		
		T = 210.0 K			
1152.40	21.595	428.05	19.904	135.86	18.770
1095.76	21.504	402.27	19.823	118.84	18.685
1041.77	21.404	377.77	19.742	105.48	18.615
989.88	21.303	354.64	19.664	95.13	18.559
940.52	21.201	332.40	19.586	87.31	18.516
892.71	21.100	311.34	19.507	82.02	18.486

Table I (*Continued*)

P/bar	ρ/ (mol L^{-1})	P/bar	ρ/ (mol L^{-1})	P/bar	ρ/ (mol L^{-1})
846.91	21.000	291.27	19.428	76.67	18.455
803.10	20.900	272.27	19.352	72.33	18.429
760.91	20.802	254.38	19.278	66.36	18.394
720.79	20.705	237.39	19.209	54.47	18.321
681.82	20.610	221.55	19.143	36.95	18.234
645.05	20.516	206.58	19.081	26.33	18.129
609.92	20.424	192.51	19.022	20.72	18.090
576.44	20.333	179.51	18.967	17.40	18.066
543.99	20.244	167.28	18.918	13.58	18.039
512.81	20.157	155.84	18.865	10.92	18.021
483.14	20.071	145.38	18.816	9.05	18.007
454.90	19.987				
		T = 220.0 K			
1307.88	21.575	519.79	19.816	151.16	18.339
1247.53	21.486	491.37	19.728	133.03	18.236
1188.75	21.392	464.27	19.642	117.66	18.143
1132.59	21.292	438.00	19.558	105.24	18.066
1079.65	21.192	413.91	19.473	95.42	18.003
1028.45	21.091	390.08	19.391	84.91	17.933
978.18	20.988	367.59	19.309	78.60	17.890
931.60	20.885	346.39	19.228	74.51	17.861
885.89	20.782	326.06	19.149	67.68	17.813
841.61	20.680	306.39	19.068	63.26	17.782
800.88	20.579	287.88	18.990	56.22	17.730
760.23	20.480	270.78	18.913	47.27	17.663
718.77	20.373	254.15	18.839	39.14	17.612
680.95	20.275	238.63	18.768	30.80	17.538
646.53	20.180	209.73	18.635	24.44	17.488
612.29	20.088	196.34	18.573	19.15	17.446
580.16	19.996	183.94	18.512	14.71	17.404
549.44	19.905	172.16	18.454	11.23	17.371
		T = 231.0 K			
1210.87	21.104	524.84	19.403	212.28	18.092
1155.60	21.002	497.39	19.313	199.61	18.026
1103.09	20.898	471.46	19.224	187.98	17.961
1052.40	20.793	446.66	19.137	166.88	17.838
1003.66	20.687	423.03	19.050	147.94	17.720
956.46	20.582	400.44	18.965	85.50	17.287
912.66	20.477	378.85	18.880	76.52	17.217
868.61	20.374	358.21	18.796	72.25	17.184
827.64	20.270	338.49	18.713	64.83	17.124
787.61	20.169	319.96	18.629	56.58	17.056
749.76	20.068	301.94	18.546	45.61	16.962
713.41	19.969	285.20	18.465	37.16	16.908
678.80	19.872	268.83	18.386	28.21	16.817
645.16	19.775	253.19	18.310	19.62	16.730
612.73	19.680	238.58	18.235	17.36	16.701
582.03	19.587	225.56	18.161	13.77	16.667
552.87	19.494				
		T = 240.0 K			
1135.21	20.720	507.48	19.026	130.40	17.101
1088.40	20.615	482.25	18.934	117.24	16.992
1035.55	20.512	458.07	18.844	103.95	16.876
989.20	20.407	435.06	18.755	94.77	16.791
944.46	20.302	413.13	18.667	87.51	16.722
901.67	20.198	391.87	18.579	81.85	16.666
860.68	20.093	371.67	18.493	77.60	16.624
821.27	19.989	352.54	18.407	74.33	16.590
782.64	19.887	316.44	18.236	71.85	16.565
746.38	19.785	299.73	18.151	66.04	16.503
711.61	19.684	268.50	17.987	62.00	16.460
677.97	19.584	240.35	17.830	55.34	16.386
645.33	19.487	227.13	17.755	46.16	16.280
614.86	19.389	203.27	17.610	35.88	16.157
584.64	19.294	181.56	17.474	29.27	16.077
557.06	19.199	162.52	17.345	23.58	16.000
529.51	19.106	145.30	17.218	20.84	15.959
		T = 250.0 K			
1112.88	20.388	459.06	18.458	173.15	16.918
1063.62	20.283	437.01	18.367	164.24	16.846
1016.28	20.283	415.77	18.278	156.05	16.777
972.11	20.176	395.75	18.190	148.40	16.710
928.29	19.957	376.74	18.103	141.38	16.645
885.92	19.846	358.62	18.016	128.27	16.518
846.02	19.738	340.55	17.931	116.85	16.399
808.55	19.631	323.35	17.846	98.54	16.190
772.26	19.526	307.58	17.759	83.78	16.002
737.40	19.423	292.49	17.675	75.45	15.888
704.17	19.322	275.39	17.576	65.88	15.748
672.71	19.220	261.39	17.494	56.26	15.599
642.10	19.120	247.72	17.415	44.88	15.408
613.16	19.023	235.34	17.336	34.77	15.316
584.71	18.926	223.41	17.260	31.46	15.240
557.82	18.830	212.31	17.185	26.70	15.153
531.73	18.735	201.56	17.113	24.71	15.107
506.45	18.641	191.54	17.041	23.27	14.965
482.52	18.549	182.15	16.971		
		T = 260.0 K			
1109.42	20.135	513.40	18.333	243.15	16.890
1062.15	20.029	490.46	18.238	232.29	16.809
1017.02	19.922	468.92	18.144	221.75	16.729
973.47	19.813	448.02	18.051	211.77	16.651
932.00	19.704	427.77	17.959	202.05	16.574
890.98	19.593	408.76	17.868	193.17	16.500
852.14	19.484	390.16	17.777	184.61	16.427
815.42	19.376	372.67	17.688	176.04	16.351
778.98	19.267	355.93	17.599	160.52	16.202
745.56	19.162	339.56	17.509	146.98	16.054
703.33	19.028	321.97	17.409	134.00	15.901
673.13	18.925	307.52	17.321	123.42	15.766
643.81	18.823	293.57	17.233	116.30	15.670
615.40	18.723	280.34	17.146	90.90	15.289
588.35	18.624	267.60	17.060	76.18	15.036
562.38	18.526	255.16	16.975	67.65	14.877
537.65	18.428				
		T = 270.2 K			
994.02	19.576	504.38	17.922	302.67	16.812
965.68	19.459	483.28	17.826	290.04	16.723
875.90	19.251	463.05	17.731	266.74	16.549
805.29	19.036	443.56	17.637	245.18	16.381
745.55	18.820	425.16	17.543	216.80	16.137
680.17	18.616	407.44	17.451	199.95	15.982
651.88	18.514	390.40	17.360	184.66	15.831
624.43	18.413	373.96	17.269	170.74	15.688
598.35	18.313	358.37	17.179	158.21	15.531
573.41	18.214	343.42	17.089	146.73	15.375
549.46	18.116	329.21	17.000	131.80	15.151
526.57	18.018	315.64	16.902	119.13	14.940
		T = 276.0 K			
1113.09	19.723	618.60	18.206	311.55	16.646
1066.37	19.614	593.22	18.105	297.45	16.542
1023.44	19.504	568.73	18.003	280.99	16.417
981.07	19.393	545.76	17.901	269.24	16.324
940.56	19.281	523.26	17.802	255.76	16.213
902.04	19.171	501.88	17.705	244.92	16.121
865.52	19.061	462.55	17.516	235.30	16.036
830.29	18.951	443.76	17.420	225.33	15.945
795.66	18.841	410.42	17.254	214.71	15.845
763.28	18.733	390.56	17.143	205.29	15.753
731.86	18.626	373.54	17.043	197.15	15.669
701.48	18.518	357.41	16.947	185.57	15.547
672.41	18.412	342.70	16.854	177.37	15.456
645.01	18.308	327.49	16.755		
		T = 280.0 K			
1110.95	19.615	602.34	18.001	309.85	16.428
1067.06	19.508	578.53	17.900	296.44	16.325
1024.53	19.398	555.27	17.800	284.29	16.229
983.89	19.287	533.04	17.701	273.60	16.139
943.80	19.175	512.19	17.602	263.18	16.049
905.55	19.064	488.98	17.492	241.46	15.857
869.11	18.954	469.28	17.395	232.83	15.772
834.79	18.845	450.03	17.296	223.80	15.684
800.76	18.734	430.61	17.192	215.64	15.600
768.93	18.627	413.65	17.097	198.67	15.421
738.20	18.520	395.49	16.992	191.54	15.340
708.83	18.415	378.13	16.889	184.89	15.262
680.95	18.310	363.25	16.796	178.31	15.182
653.51	18.206	348.51	16.700	165.32	14.984
627.42	18.104	335.06	16.609		

Table II. Coefficients A_1 to A_{16} and Gas Constant R for Eq 1

$A_1 = -0.84538639 \times 10^0$ dm^3 mol^{-1}
$A_2 = +0.37111568 \times 10^2$ bar dm^6 mol^{-2}
$A_3 = -0.47852387 \times 10^4$ bar dm^6 K mol^{-2}
$A_4 = +0.48240806 \times 10^6$ bar dm^6 K^2 mol^{-2}
$A_5 = -0.21576945 \times 10^{10}$ bar dm^6 K^4 mol^{-2}
$A_6 = +0.55019161 \times 10^{-1}$ dm^6 mol^{-2}
$A_7 = -0.16151426 \times 10^1$ bar dm^9 mol^{-3}
$A_8 = -0.48170718 \times 10^{-4}$ bar dm^{12} K^{-1} mol^{-3}
$A_9 = -0.12136652 \times 10^6$ bar dm^9 K^2 mol^{-3}
$A_{10} = +0.25284349 \times 10^8$ bar dm^9 K^3 mol^{-3}
$A_{11} = -0.14967567 \times 10^{10}$ bar dm^9 K^4 mol^{-3}
$A_{12} = +0.38784395 \times 10^3$ bar dm^{15} K^2 mol^{-5}
$A_{13} = -0.86096236 \times 10^5$ bar dm^{15} K^3 mol^{-5}
$A_{14} = +0.55120465 \times 10^7$ bar dm^{15} K^4 mol^{-5}
$A_{15} = +0.46546609 \times 10^{-4}$ bar dm^{18} mol^{-6}
$A_{16} = -0.40000000 \times 10^{-2}$ dm^6 mol^{-2}
$R = 0.083144$ dm^3 bar K^{-1} mol^{-1}

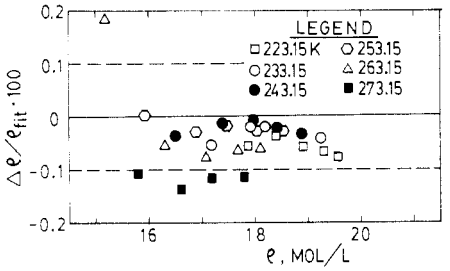

Figure 4. Relative deviations in density of the IUPAC data (*1*) from eq 1 of this work. The dashed lines represent one standard deviation in the fitted data.

the limits of the absolute accuracy estimated for our experimental method (≃0.1%) and within the standard deviation of eq 1 (0.1%). It should be noted that the experimental method used here is accurate only for the measurement of densities higher than about twice the critical density (≃15 mol dm^{-3} for ethylene).

Thermodynamic Properties

With the constants A_i given in Table II we have calculated thermodynamic properties of the saturated and compressed liquid by applying known thermodynamic relations to eq 1.

Gas and Saturated-Liquid Properties. To obtain the configurational internal energy U_s^c of the saturated liquid, we have used the following equation:

$$U_s^c = -\Delta H_v + RT\left[\left(B - T\frac{dB}{dT}\right)/V_{vap} + \left(2C - T\frac{dC}{dT}\right)/2V_{vap}^2\right] + RT - PV_{liq} \quad (2)$$

Here ΔH_v is the enthalpy of vaporization at saturation. The second term in eq 2 corrects ΔH_v to the condition of the ideal gas in the vapor phase. Its calculation requires knowledge of the second virial coefficient B, the third virial coefficient C, and their temperature derivatives, as well as the molar volume of the saturated vapor V_{vap} which can be obtained from the virial equation of state:

$$PV = RT\left[1 + \frac{1}{V_{vap}}B + \frac{1}{V_{vap}^2}C + \ldots\right] \quad (3)$$

The molar volume of the liquid, V_{liq}, has been calculated by extrapolation of eq 1 to the pressure P of the saturated liquid. The Clausius–Clapeyron equation has been used to obtain ΔH_v:

$$\Delta H_v = T(dP/dT)_{sat}(V_{vap} - V_{liq}) \quad (4)$$

The saturation pressure, P, and its temperature derivative have

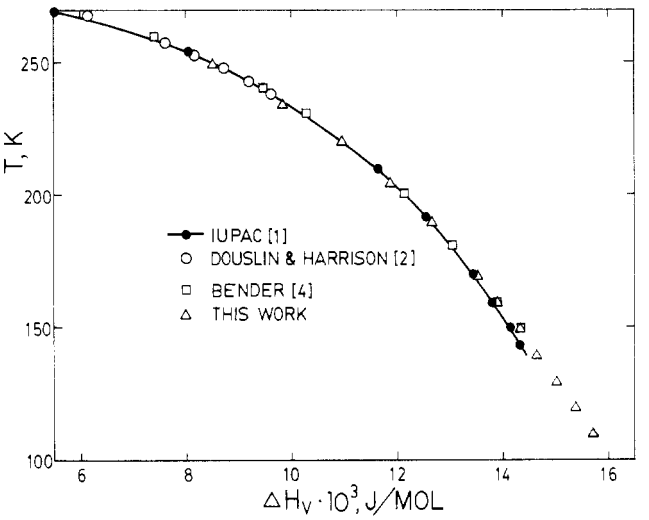

Figure 5. Enthalpy of vaporization of ethylene: comparison with published data.

been calculated up to 235 K from the vapor pressure equation published by the IUPAC commission (*1*). Above 235 K the Cox equation, which gives very accurate pressure values with parameters fitted by Douslin and Harrison (*2*), has been used. Reliable experimental data for the second virial coefficient B are only available for temperatures above 220 K. To obtain values of B at lower temperatures, we have used a relation given by McGlashan and Potter, which has proved to give a good representation of B for saturated hydrocarbons and α-olefins up to eight carbon atoms (*15*, *16*):

$$B = V_c[0.430 - 0.886(T/T_c)^{-1} - 0.694(T/T_c)^{-2} - 0.0375(n-1)(T/T_c)^{-4.5}] \quad (5)$$

Here n is approximately the number of carbon atoms, V_c is the critical volume, and T_c is the critical temperature of the liquid. With $V_c = 130.98$ cm^3 mol^{-1} for ethylene, $n = 2.2$ has been found to give the best fit to the data of both Michels and Geldermans (*17*) and Douslin and Harrison (*2*), which have been regarded as the most reliable. Equation 5 has been used for calculation of B at temperatures below 220 K and for calculation of dB/dT. Only a few experimental measurements have been reported for the third virial coefficient C. To represent the data reported by Douslin and Harrison (*2*), we used the equation proposed by Chueh and Prausnitz (*18*) for a fitting procedure ($T_R = T/T_c$):

$$\frac{C}{V_c^2} = (0.232T_R^{-0.25} + 0.468T_R^{-5})(1 - \exp[1 - 1.89T_R^2]) + d\exp[-(2.49 - 2.30T_R + 2.70T_R^2)] \quad (6)$$

The parameter d equals zero for rare gases and should be greater for molecules with nonspherical shape. For ethylene $d = 0.59$ has been found to give a best fit and eq 6 has also been used for calculating dC/dT. According to the recommendation of Chueh and Prausnitz, eq 6 has been set to zero at temperatures lower than 210 K where C becomes negative and eq 6 is no longer applicable. The influence of this truncation is negligible as the vapor densities are low at temperatures below 210 K, and C in eq 3 can be ignored under these conditions.

The results of these calculations are summarized in Table III. In Figure 5 the results of ΔH_v are compared with those of other authors. The agreement at high temperatures with the data of Douslin and Harrison (*2*), who used direct PVT data of the saturated liquid and vapor in applying the Clausius–Clapeyron equation, is remarkably good considering that our calculation of the molar volume of the vapor is based on eq 3,

Table III. Thermodynamic Properties of Liquid and Gaseous Ethylene at Saturation

T/K	P/bar	B/(cm³ mol⁻¹)	C/(cm⁶ mol⁻¹)	V_{vap}/(cm³ mol⁻¹)	V_{liq}/(cm³ mol⁻¹)	ΔH_v/(J mol⁻¹)	$-U_s^c$/(J mol⁻¹)
110	0.0033	−1250.4			43.33	15 738	14 825
120	0.0136	−997.1			44.21	15 385	14 393
130	0.0442	−818.0		243920	45.15	15 021	13 953
140	0.1184	−685.9		97627	46.15	14 655	13 519
150	0.2736	−585.7		44983	47.19	14 286	13 093
160	0.5623	−507.5		23142	48.29	13 908	12 673
170	1.0510	−445.0		12988	49.48	13 512	12 256
180	1.8191	−394.1		7812	50.79	13 900	11 837
190	2.9562	−351.9		4965	52.19	12 633	11 412
205	5.5673	−300.8		2723.3	54.61	11 855	10 753
220	9.5771	−260.5	5383	1603.8	57.54	10 955	10 090
235	15.3520	−227.8	7325	989.2	61.24	9 841	9 341
250	23.3003	−200.9	7976	622.6	66.67	8 521	8 592

Table IV. Mechanical and Adiabatic Coefficients for Saturated Liquid Ethylene on the Liquid-Vapor Coexistence Curve

T/K	$10^4\beta_T$/bar⁻¹	$10^3\alpha_P$/K⁻¹	γ_V/(bar K⁻¹)	γ_σ/(bar K⁻¹)	$10^3\alpha_\sigma$/K⁻¹
110	0.81	1.93	23.69	0.00	1.93
120	0.91	2.06	22.54	0.00	2.06
130	1.04	2.14	20.49	0.00	2.13
140	1.20	2.20	18.43	0.01	2.20
150	1.38	2.28	16.58	0.02	2.28
160	1.59	2.38	14.98	0.04	2.38
170	1.85	2.51	13.57	0.06	2.50
180	2.17	2.68	12.31	0.09	2.65
190	2.58	2.88	11.16	0.14	2.84
205	3.44	3.29	9.55	0.22	3.21
220	4.87	3.92	8.04	0.32	3.76
235	7.71	5.04	6.54	0.45	4.69
250	16.68	8.26	4.95	0.61	7.24

where terms of higher order than C/V_{vap}^2 have been excluded. Data of other authors also show good agreement in this temperature range. At low temperatures our data are in close agreement with Bender's results, whose equation of state was fitted to both the liquid and vapor region (*4*). However, the IUPAC equation for ΔH_v, based on direct calorimetric data (*19*), gives systematically lower values than those reported here at temperatures below 170 K.

The following mechanical coefficients for the saturated liquid have been calculated from eq 1: the isothermal compressibility, $\beta_T = -1/V(\partial V/\partial P)_T$; the thermal expansion coefficient, $\alpha_P = 1/V(\partial V/\partial P)_T$; and the thermal pressure coefficient, $\gamma_V = (\partial P/\partial T)_V$. The thermal expansion coefficient along the saturation line, α_σ, has been calculated from the equation

$$\alpha_\sigma = \alpha_P(1 - \gamma_\sigma/\gamma_V) \tag{7}$$

where γ_σ is the gradient of the vapor pressure curve dP/dT. The mechanical coefficients are recorded in Table IV.

Compressed-Liquid Properties. Equation 1 has been used to derive values of density at regular intervals of pressure, as recorded in Table V. For the same pressures, values of β_T, α_P, γ_V, the configurational internal energy, U^c, and the entropy S^c, relative to the entropy of the ideal gas at the same density ρ have been calculated and are recorded in Tables VI–X. Values of U^c in Table IX have been calculated from

$$U^c = U_s^c + \int_{V_{ig}}^{V} [T(\partial P/\partial T)_V - P]\, dV \tag{8}$$

using values of U_s^c from Table III. The relative entropy S^c in Table X has been calculated from

$$S^c = \int_{V_{ig}}^{V} \left(\frac{\partial P}{\partial T}\right)_V dV + R \ln \frac{\rho_{liq}}{\rho_{vap}} - \left[\left(B + T\frac{dB}{dT}\right)\rho_{vap} + \tfrac{1}{2}\left(C + T\frac{dC}{dT}\right)\rho_{vap}^2\right] - \frac{\Delta H_v}{T} \tag{9}$$

Fluid Properties at the Melting Curve. Straty (*5*) has reported a fit of the Simon equation to his experimental results for the melting pressure up to 360 bar. Densities and mechanical coefficients for liquid ethylene along the melting curve at 110 and 120 K are recorded in Table XI. The reliability of the data calculated depends on the validity of the Simon equation extrapolated to pressures above 360 bar. Hence, these results should be regarded as approximate.

Theoretical Calculations

For ethylene, as for all but the simplest molecules, the intermolecular pair potential, $U(r\omega_1\omega_2)$, depends on the molecular

Table V. Density ρ of Ethylene (mol dm⁻³)

P/bar \ T, K	110	120	130	140	150	160	170	180	190	205	220	235	250	265	280
5	23.085	22.628	22.160	21.686	21.207	20.721	20.222	19.707	19.170						
10	23.094	22.639	22.171	21.699	21.222	20.737	20.241	19.728	19.195	18.340	17.388				
15	23.103	22.649	22.182	21.711	21.236	20.753	20.259	19.749	19.219	18.371	17.430				
25	23.122	22.669	22.205	21.737	21.264	20.785	20.295	19.791	19.267	18.431	17.511	16.446	15.039		
50	23.168	22.719	22.261	21.799	21.334	20.864	20.384	19.891	19.382	18.576	17.700	16.717	15.532		
100	23.257	22.817	22.369	21.920	21.468	21.013	20.552	20.080	19.596	18.839	18.034	17.165	16.200	15.066	
200	23.428	23.003	22.573	22.145	21.717	21.289	20.857	20.420	19.975	19.292	18.583	17.848	17.081	16.280	15.441
300	23.590	23.177	22.763	22.352	21.945	21.538	21.130	20.720	20.306	19.675	19.031	18.376	17.710	17.038	16.366
400	23.743	23.341	22.940	22.545	22.154	21.766	21.378	20.990	20.600	20.009	19.414	18.814	18.213	17.616	17.028
500		23.496	23.107	22.725	22.349	21.977	21.606	21.236	20.865	20.308	19.749	19.191	18.636	18.090	17.556
600		23.643	23.265	22.895	22.531	22.173	21.816	21.462	21.108	20.578	20.049	19.523	19.004	18.495	18.001
700		23.783	23.414	23.055	22.703	22.356	22.013	21.672	21.332	20.825	20.321	19.822	19.331	18.852	18.388
800		23.917	23.556	23.206	22.865	22.529	22.197	21.867	21.540	21.053	20.570	20.094	19.627	19.171	18.731
900		24.045	23.692	23.351	23.018	22.692	22.370	22.051	21.735	21.265	20.801	20.344	19.896	19.461	19.040
1000		24.168	23.822	23.489	23.164	22.847	22.534	22.225	21.918	21.464	21.016	20.575	20.145	19.726	19.322
1100		24.287	23.947	23.620	23.304	22.994	22.689	22.389	22.091	21.651	21.217	20.791	20.375	19.972	19.582
1200		24.401	24.067	23.747	23.437	23.135	22.838	22.545	22.255	21.827	21.406	20.994	20.591	20.200	19.824
1300			24.182	23.868	23.565	23.269	22.979	22.694	22.412	21.995	21.585	21.184	20.794	20.415	20.049

Table VI. Isothermal Compressibility β_T of Ethylene $\times 10^4$ (bar^{-1})

P/bar \ T, K	110	120	130	140	150	160	170	180	190	205	220	235	250	265	280
5	0.81	0.91	1.04	1.19	1.37	1.58	1.84	2.16	2.57						
10	0.81	0.91	1.03	1.18	1.36	1.57	1.82	2.14	2.54	3.39	4.86				
15	0.80	0.90	1.03	1.18	1.35	1.56	1.81	2.12	2.51	3.34	4.75				
25	0.80	0.89	1.02	1.16	1.33	1.53	1.78	2.07	2.45	3.24	4.54	7.14	16.04		
50	0.78	0.88	0.99	1.13	1.29	1.48	1.71	1.98	2.32	3.01	4.09	6.03	10.67		
100	0.76	0.84	0.95	1.07	1.22	1.38	1.58	1.81	2.09	2.64	3.44	4.67	6.84	11.67	
200	0.71	0.78	0.87	0.97	1.09	1.23	1.38	1.56	1.76	2.14	2.64	3.31	4.23	5.54	7.50
300	0.67	0.73	0.80	0.89	0.99	1.10	1.23	1.37	1.53	1.81	2.16	2.59	3.13	3.81	4.64
400	0.63	0.68	0.75	0.83	0.91	1.00	1.11	1.22	1.35	1.57	1.84	2.15	2.51	2.94	3.43
500		0.64	0.70	0.77	0.84	0.92	1.01	1.11	1.21	1.39	1.60	1.84	2.11	2.41	2.74
600		0.61	0.66	0.72	0.78	0.85	0.93	1.01	1.10	1.25	1.42	1.61	1.82	2.05	2.29
700		0.58	0.62	0.68	0.73	0.80	0.86	0.93	1.01	1.14	1.28	1.43	1.60	1.78	1.97
800		0.55	0.59	0.64	0.69	0.74	0.80	0.87	0.93	1.04	1.16	1.29	1.43	1.58	1.73
900		0.52	0.56	0.60	0.65	0.70	0.75	0.81	0.87	0.96	1.07	1.18	1.30	1.42	1.55
1000		0.50	0.53	0.57	0.62	0.66	0.71	0.76	0.81	0.90	0.99	1.09	1.19	1.29	1.40
1100		0.48	0.51	0.55	0.58	0.63	0.67	0.71	0.76	0.84	0.92	1.00	1.09	1.19	1.28
1200		0.46	0.49	0.52	0.56	0.59	0.63	0.68	0.72	0.79	0.86	0.94	1.01	1.09	1.17
1300			0.47	0.50	0.53	0.57	0.60	0.64	0.68	0.74	0.81	0.88	0.95	1.02	1.09

Table VII. Thermal Expansion Coefficient α_P of Ethylene $\times 10^3$ (K^{-1})

P/bar \ T, K	110	120	130	140	150	160	170	180	190	205	220	235	250	265	280
5	1.92	2.05	2.13	2.19	2.27	2.37	2.50	2.66	2.87						
10	1.92	2.05	2.12	2.19	2.26	2.36	2.49	2.65	2.85	3.26	3.91				
15	1.91	2.04	2.11	2.18	2.25	2.35	2.47	2.63	2.82	3.22	3.85				
25	1.91	2.03	2.10	2.16	2.24	2.33	2.45	2.59	2.78	3.15	3.72	4.77	8.01		
50	1.89	2.00	2.07	2.12	2.19	2.28	2.38	2.52	2.68	3.00	3.47	4.22	5.85		
100	1.85	1.95	2.01	2.05	2.11	2.18	2.27	2.38	2.51	2.76	3.08	3.54	4.24	5.62	
200	1.78	1.87	1.90	1.93	1.97	2.02	2.08	2.16	2.25	2.40	2.59	2.80	3.06	3.35	3.70
300	1.73	1.79	1.81	1.83	1.85	1.89	1.93	1.99	2.05	2.16	2.28	2.40	2.52	2.64	2.73
400	1.68	1.73	1.73	1.74	1.76	1.78	1.81	1.85	1.90	1.98	2.05	2.13	2.20	2.25	2.27
500		1.67	1.67	1.67	1.67	1.69	1.71	1.74	1.78	1.83	1.89	1.94	1.97	1.99	1.99
600		1.62	1.61	1.60	1.60	1.61	1.63	1.65	1.68	1.72	1.75	1.79	1.81	1.81	1.80
700		1.57	1.55	1.54	1.54	1.54	1.55	1.57	1.59	1.62	1.65	1.67	1.68	1.67	1.65
800		1.53	1.51	1.49	1.48	1.48	1.49	1.50	1.51	1.54	1.55	1.57	1.57	1.56	1.54
900		1.50	1.46	1.44	1.43	1.43	1.43	1.44	1.45	1.46	1.48	1.48	1.48	1.47	1.44
1000		1.46	1.42	1.40	1.38	1.38	1.38	1.38	1.39	1.40	1.41	1.41	1.41	1.39	1.37
1100		1.43	1.39	1.36	1.34	1.33	1.33	1.34	1.34	1.35	1.35	1.35	1.34	1.32	1.30
1200		1.40	1.36	1.32	1.30	1.29	1.29	1.29	1.29	1.30	1.30	1.30	1.28	1.27	1.24
1300			1.33	1.29	1.27	1.26	1.25	1.25	1.25	1.25	1.25	1.25	1.23	1.22	1.19

Table VIII. Thermal Pressure Coefficient γ_V of Ethylene (bar K^{-1})

P/bar \ T, K	110	120	130	140	150	160	170	180	190	205	220	235	250	265	280
5	23.73	22.58	20.53	18.46	16.62	15.01	13.61	12.34	11.18						
10	23.76	22.61	20.56	18.50	16.66	15.05	13.65	12.38	11.22	9.60	8.04				
15	23.80	22.65	20.60	18.54	16.70	15.09	13.69	12.43	11.27	9.65	8.10				
25	23.87	22.71	20.67	18.61	16.77	15.17	13.77	12.51	11.36	9.75	8.21	6.68	4.99		
50	24.05	22.89	20.84	18.79	16.96	15.37	13.97	12.72	11.57	9.98	8.48	7.01	5.49		
100	24.41	23.23	21.18	19.14	17.32	15.74	14.36	13.12	11.99	10.42	8.96	7.57	6.20	4.82	
200	25.17	23.91	21.86	19.82	18.01	16.45	15.08	13.85	12.74	11.21	9.81	8.49	7.24	6.05	4.94
300	25.95	24.60	22.51	20.47	18.66	17.10	15.74	14.53	13.43	11.92	10.54	9.25	8.05	6.92	5.88
400	26.75	25.28	23.14	21.09	19.28	17.72	16.36	15.15	14.06	12.56	11.19	9.92	8.74	7.64	6.63
500		25.96	23.76	21.68	19.87	18.31	16.95	15.74	14.64	13.15	11.79	10.53	9.36	8.27	7.27
600		26.63	24.37	22.26	20.43	18.86	17.50	16.29	15.19	13.70	12.34	11.09	9.92	8.84	7.84
700		27.30	24.96	22.82	20.97	19.39	18.03	16.81	15.71	14.22	12.86	11.61	10.45	9.37	8.37
800		27.96	25.54	23.36	21.49	19.90	18.53	17.31	16.21	14.72	13.36	12.10	10.94	9.86	8.86
900		28.62	26.11	23.88	21.99	20.39	19.01	17.79	16.69	15.19	13.83	12.57	11.40	10.32	9.32
1000		29.28	26.67	24.39	22.48	20.86	19.47	18.25	17.14	15.64	14.27	13.01	11.85	10.76	9.75
1100		29.93	27.22	24.89	22.95	21.32	19.92	18.69	17.58	16.07	14.70	13.44	12.27	11.18	10.17
1200		30.58	27.76	25.38	23.41	21.76	20.35	19.11	18.00	16.49	15.11	13.85	12.67	11.58	10.57
1300			28.29	25.85	23.86	22.19	20.77	19.53	18.41	16.89	15.51	14.24	13.07	11.97	10.95

orientations ω_i ($=\theta\phi_i\chi_i$ for nonlinear molecules) as well as the intermolecular separation r. Such a potential may be separated into isotropic and anisotropic parts, as suggested originally by Pople (*20*):

$$U(r\omega_1\omega_2) = U_0(r) + U_a(r\omega_1\omega_2) \quad (10)$$

where U_0 is a reference pair potential of isotropic particles and U_a contains all of the orientation-dependent terms. The Pople reference potential is given by

$$U_0(r) = \langle U(r\omega_1\omega_2)\rangle_{\omega_1\omega_2} \quad (11)$$

where $\langle ... \rangle$ denotes an unweighted average over orientations ω_i. Gubbins and Gray have developed a perturbation theory (*7*, *21*) in which the Pople reference is employed to obtain the thermodynamic properties of anisotropic fluids.

The Helmholtz free energy, A, may be expanded as

$$A = A_0 + A_1 + A_2 + A_3 + ... \quad (12)$$

With the choice of a Pople reference, the first-order term A_1 disappears. Expressions for the second- and third-order terms, A_2 and A_3, have been developed for various anisotropic interactions (e.g., multipolar, overlap, and dispersion), and these are

Table IX. Configurational Internal Energy U^c of Ethylene (J mol^{-1})

P/bar \ T, K	110	120	130	140	150	160	170	180	190	205	220	235	250
5	−14 829	−14 398	−13 959	−13 526	−13 100	−12 681	−12 264	−11 844	−11 417				
10	−14 834	−14 403	−13 965	−13 533	−13 108	−12 690	−12 274	−11 856	−11 431	−10 769	−10 091		
15	−14 838	−14 408	−13 971	−13 540	−13 116	−12 699	−12 284	−11 868	−11 445	−10 787	−10 116		
25	−14 847	−14 419	−13 984	−13 554	−13 132	−12 717	−12 305	−11 892	−11 473	−10 822	−10 163	−9 408	−8 614
50	−14 869	−14 446	−14 014	−13 588	−13 170	−12 760	−12 354	−11 949	−11 539	−10 906	−10 273	−9 563	−8 883
100	−14 912	−14 496	−14 071	−13 653	−13 243	−12 843	−12 448	−12 055	−11 661	−11 057	−10 466	−9 818	−9 250
200	−14 993	−14 591	−14 178	−13 772	−13 377	−12 992	−12 616	−12 244	−11 874	−11 315	−10 780	−10 205	−9 737
300	−15 068	−14 678	−14 276	−13 880	−13 496	−13 124	−12 763	−12 407	−12 056	−11 529	−11 031	−10 500	−10 083
400	−15 138	−14 758	−14 365	−13 978	−13 604	−13 243	−12 893	−12 551	−12 215	−11 713	−11 243	−10 741	−10 355
500		−14 832	−14 446	−14 067	−13 702	−13 350	−13 010	−12 680	−12 356	−11 873	−11 424	−10 945	−10 581
600		−14 901	−14 522	−14 150	−13 791	−13 448	−13 117	−12 796	−12 482	−12 015	−11 584	−11 122	−10 775
700		−14 966	−14 592	−14 226	−13 873	−13 537	−13 213	−12 901	−12 595	−12 143	−11 725	−11 278	−10 944
800		−15 026	−14 658	−14 296	−13 949	−13 619	−13 302	−12 997	−12 699	−12 258	−11 853	−11 417	−11 093
900		−15 083	−14 719	−14 361	−14 020	−13 695	−13 384	−13 085	−12 794	−12 363	−11 968	−11 542	−11 228
1000		−15 136	−14 776	−14 422	−14 085	−13 765	−13 459	−13 166	−12 881	−12 460	−12 073	−11 656	−11 349
1100		−15 187	−14 829	−14 479	−14 146	−13 830	−13 529	−13 241	−12 961	−12 548	−12 170	−11 760	−11 459
1200		−15 234	−14 880	−14 533	−14 203	−13 891	−13 594	−13 311	−13 035	−12 630	−12 259	−11 855	−11 560
1300			−14 927	−14 583	−14 256	−13 947	−13 655	−13 375	−13 105	−12 705	−12 341	−11 943	−11 653

Table X. Entropy S^c of Liquid Ethylene Relative to the Ideal Gas at the Same Density (J mol^{-1} K^{-1})

P/bar \ T, K	110	120	130	140	150	160	170	180	190	205	220	235	250
5	−51.11	−47.52	−44.17	−41.14	−38.39	−35.87	−33.54	−31.35	−29.27				
10	−51.14	−47.56	−44.22	−41.18	−38.43	−35.92	−33.59	−31.41	−29.33	−26.35	−23.59		
15	−51.18	−47.60	−44.26	−41.23	−38.48	−35.97	−33.65	−31.47	−29.40	−26.42	−23.68		
25	−51.26	−47.68	−44.35	−41.32	−38.58	−36.07	−33.75	−31.58	−29.52	−26.57	−23.86	−21.03	−18.45
50	−51.45	−47.89	−44.56	−41.54	−38.81	−36.31	−34.01	−31.86	−29.83	−26.92	−24.28	−21.57	−19.28
100	−51.82	−48.28	−44.98	−41.97	−39.26	−36.79	−34.51	−32.39	−30.40	−27.57	−25.04	−22.48	−20.48
200	−52.53	−49.05	−45.77	−42.79	−40.11	−37.67	−35.44	−33.37	−31.44	−28.72	−26.32	−23.94	−22.17
300	−53.22	−49.78	−46.52	−43.56	−40.89	−38.48	−36.28	−34.26	−32.37	−29.72	−27.41	−25.13	−23.46
400	−53.89	−50.48	−47.23	−44.28	−41.63	−39.24	−37.07	−35.07	−33.21	−30.62	−28.37	−26.15	−24.54
500		−51.14	−47.91	−44.97	−42.33	−39.95	−37.80	−35.82	−33.99	−31.44	−29.23	−27.05	−25.47
600		−51.79	−48.56	−45.62	−42.99	−40.63	−38.49	−36.53	−34.72	−32.20	−30.02	−27.86	−26.31
700		−52.41	−49.18	−46.25	−43.62	−41.27	−39.14	−37.20	−35.40	−32.90	−30.75	−28.61	−27.08
800		−53.02	−49.78	−46.85	−44.22	−41.88	−39.76	−37.83	−36.04	−33.57	−31.43	−29.31	−27.78
900		−53.60	−50.36	−47.43	−44.80	−42.46	−40.35	−38.43	−36.65	−34.19	−32.07	−29.96	−28.44
1000		−54.17	−50.93	−47.98	−45.36	−43.02	−40.91	−39.00	−37.23	−34.78	−32.68	−30.57	−29.06
1100		−54.73	−51.47	−48.52	−45.90	−43.56	−41.46	−39.55	−37.79	−35.35	−33.25	−31.15	−29.64
1200		−55.27	−52.00	−49.04	−46.42	−44.08	−41.98	−40.07	−38.32	−35.89	−33.80	−31.71	−30.19
1300			−52.52	−49.55	−46.92	−44.58	−42.48	−40.58	−38.83	−36.41	−34.32	−32.23	−30.72

Table XI. Densities and Mechanical Coefficients for Saturated Liquid Ethylene on the Melting Curve

T/K	P/bar	ρ/(mol L^{-1})	$10^4 \cdot \beta_T$/bar^{-1}	$10^3 \cdot \alpha_P$/K^{-1}	γ_V/(bar K^{-1})	γ_σ/(bar K^{-1})	$10^3 \cdot \alpha_\sigma$/K^{-1}
110	440.5	23.80	0.62	1.67	27.08	75.44	−2.98
120	1231.6	24.44	0.45	1.40	30.78	82.77	−2.36

fully described in earlier publications (*7*, *20*, *21*). The slow convergence of eq 12 is greatly improved by using a Padé approximant as suggested by Stell (*22*)

$$A = A_0 + A_2(1 - A_3/A_2)^{-1} \quad (13)$$

This closure provides excellent agreement between the theory and computer simulation for even highly polar fluids (such as water). Extensive comparisons of the free energy obtained by using eq 13, and other derived thermodynamic properties, with those for real fluids have also been made with considerable success (*23*–*25*).

The properties of the reference system were calculated following the procedure outlined in previous publications. Briefly, the properties of the *n*–6 fluid are related to those of a 12–6 fluid using perturbation theory and then the 12–6 mixture properties are related to those of a 12–6 pure fluid using van der Waals one-fluid theory. In all of the potential models chosen the equation of state for argon due to Gosman et al. (*26*) was used as an approximation to the free energy of the 12–6 fluid. The reference fluid integrals $J_{\alpha\beta}$, $K_{\alpha\beta\gamma}$, and $L_{\alpha\beta\gamma}$ were calculated as described previously, being fitted to an expansion in reduced density and temperature as described by Twu et al. (*27*).

Potential Models. Ethylene is of special interest to theorists as one of the simplest molecules possessing a nonaxial quadrupole moment ($Q_{xx} \neq Q_{yy} \neq Q_{zz}$). Recently it has been shown (*8*) that, within the framework of the perturbation theory described earlier, the inclusion of a full nonaxial treatment of ethylene's quadrupolar interactions gives significantly better agreement with experiment for supercritical dense-fluid properties than the popular "axial" approximation (using Q_{zz} alone). The "effective axial" approximation

$$\langle Q^2 \rangle = 2/3(Q_{xx}^2 + Q_{yy}^2 + Q_{zz}^2) \quad (14)$$

gives results essentially identical with those found with the nonaxial treatment (though this is atypical of most molecules, especially polar ones) since the two independent "quadrupole" moments happen to have the same magnitude. It was pointed out (*8*) that, while the effective axial approximation will be good for *pure* ethylene, it may be poor for ethylene-containing mixtures. These points are discussed in detail in ref *8*.

Since we are concerned here only with pure-fluid properties, we are able to use the much simpler form of the effective axial model for the quadrupolar interactions of ethylene without loss of accuracy in the prediction of the thermodynamic properties. In this investigation we are interested in determining the ability of various potential models to predict the pressure dependence of certain key properties over as wide a range as possible in the subcritical dense-fluid region. In particular it will be of interest to note how the addition of anisotropic forces changes

Table XII. Potential Parameters

model	(ϵ/k)/K	σ/Å	n	$10^{26}Q$/ (esu cm^2)	κ	δ_2
A	241.8[a]	4.091[a]	13.0[a]			
B	223.9[b]	4.147[b]	13.0[b]	4.09[d]		
C	224.8[a]	4.138[a]	13.0[a]	4.09[d]	0.143[e]	
D	224.2[c]	4.140[c]	13.0[c]	4.09[d]	0.143[e]	0.10[c]
M	224.0[c]	4.137[c]	13.0[c]	3.54[f]	0.143[e]	0.10[c]

[a] Reference 24. [b] Reference 8. [c] This work. [d] "Effective axial" approximation for the quadrupole moment, ref 28. [e] Reference 29. [f] "Effective axial" approximation for the quadrupole moment, ref 31.

the comparison with experiment over that produced by a spherical Lennard-Jones model where angle-dependent forces are ignored. It was stated in ref 8 that anisotropic overlap and dispersion forces gave a negligible contribution to the supercritical dense-fluid properties; the validity of this statement in the subcritical region was also tested.

Accordingly, four potential models were used in the investigation. The full anisotropic model used may be written as

$$U = \underbrace{U_0^{(n,6)}}_{A} + \underbrace{U_{QQ}(224)}_{B} + \underbrace{U_{dis}(202 + 022 + 224)}_{C} + \underbrace{U_{ov}(202 + 022)}_{D} \quad (15)$$

where $U_0^{(n,6)}$ is the isotropic Lennard-Jones n–6 potential, $U_{QQ}(224)$ is the leading term in the multipolar series for quadrupolar interactions, and U_{dis} and U_{ov} are the leading terms in a spherical harmonic expansion for the anisotropic dispersion and overlap potentials, respectively. In model A eq 15 was truncated after the first term giving a potential model ignoring all angle-dependent terms. For model B, eq 15 was truncated after the second term; this potential is the one used in eq 42 of ref 8. Here an "effective axial" quadrupolar interaction is included but anisotropic overlap and dispersion forces are ignored. The potential for model C is given by the first three terms of eq 15, ignoring only overlap forces. Model D has the full potential given by eq 15. In this stepwise fashion the effect of each term on the thermodynamic properties may be explored. The multipole moments and anisotropic polarizabilities were available from experimental determinations. The adjustable potential parameters (ϵ, σ, n, δ_2 where applicable) given in Table XII were determined to be those giving the best fit to saturated-liquid data as has been described earlier (8); δ_2 is a shape parameter involved in the overlap potential which is constrained to lie within the range $0 < \delta_2 < 0.5$. The potential parameters thus obtained from fitting to the coexistence region were kept unaltered to predict the dense-fluid properties. The properties of the reference fluid in all of these models were calculated from the equation of state for argon due to Gosman et al. (26). The effect of changing this to the equation of state for methane (30) on the prediction of the one-fluid properties was investigated. New potential parameters for model D, the full anisotropic model, with a methane reference were obtained by fitting to the coexistence curve as before. The parameters for this potential, designated model M, are given in Table XII. A slightly different value of the effective axial quadrupole moment was used for model M, which makes use of the most recent values of Q_{xx}, Q_{yy}, and Q_{zz} (31); this does not however have any significant influence on the results.

Results. The properties of density and configurational energy and entropy were calculated, by using the models outlined in the previous section, for as wide a range of temperature and pressure as the reference equation of state would allow (i.e., densities up to $\rho\sigma^3 = 0.88$ for models with an argon reference or up to $\rho\sigma^3 = 1.0$ for model M with a methane reference). The values obtained were then compared with the experimental values given in this work. These results are shown graphically

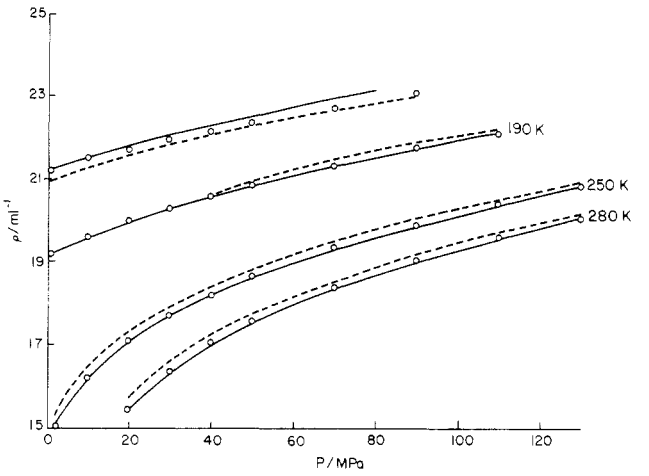

Figure 8. Comparison of experimental density values (points) with those predicted by models M (solid line) and A (dashed line) as a function of pressure for the T = 150, 190, 250, and 280 K isotherms.

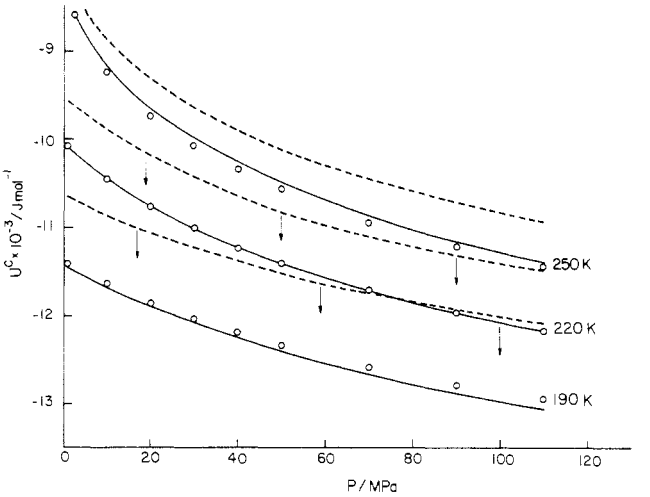

Figure 7. Comparison of experiment and theory for the configurational internal energy as a function of pressure for the T = 190, 220, and 250 K isotherms. Key as for Figure 6.

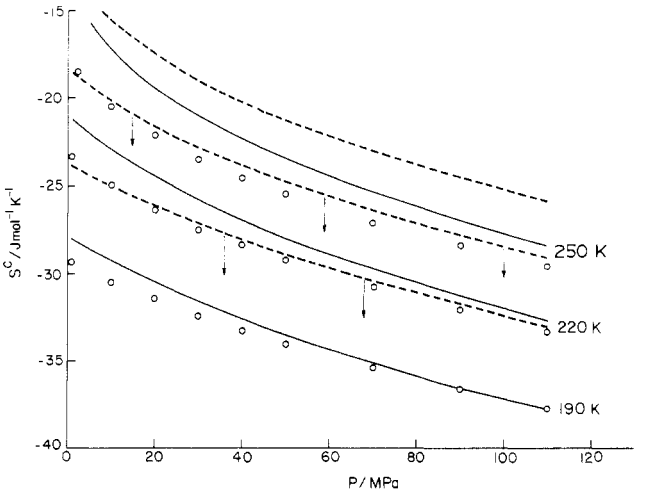

Figure 8. Comparison of experiment and theory for the configurational entropy (relative to the ideal gas at the same density) as a function of pressure for the T = 190, 220, and 250 K isotherms. Key as for Figure 6.

Table XIII. Average Percentage Deviation between Theory and Experiment[a]

model	$\|\Delta\rho\|$/%	$\|\Delta U^c\|$/%	$\|\Delta S^c\|$/%
A	0.64	4.90	16.0
B	0.59	1.30	4.7
C	0.45	0.61	4.7
D	0.40	0.63	4.3
M	0.11	0.40	5.0

[a] Range 190-280 K, $P \simeq 5$-1300 bar.

in Figures 6-8. The average percentage difference between theory and experiment over the whole range of temperature and pressure studied (roughly 190-280 K, for pressures 0.5-130.0 MPa) was evaluated for each model, as shown in Table XIII. This table clearly shows that, as the various anisotropic interactions were included in the potential model, from model A to model D, the discrepancy between theory and experiment is diminished, suggesting that the successive changes in the potential model constitute an improving refinement toward the effective potential of the real fluid. The biggest improvement overall was found between models A and B, especially for the entropy and internal energy; this is not unexpected as the addition of multipolar forces commonly provides an order of magnitude larger contribution to the free energy than either the overlap or dispersion forces. However, these latter forces are shown to provide a nonnegligible improvement to the thermodynamic properties, in contrast to that found for the supercritical region. This may indicate that the subcritical dense-fluid region is more sensitive than either the saturation curve or the supercritical dense-fluid region to more subtle interactions, represented here by the overlap and dispersion forces. The overall generally poor behavior of the isotropic model (A) indicates the importance of the angle-dependent forces as represented by models B-D.

The results for model M (potential model D with a methane reference system) given in Table XIII show this to be the overall most successful model in predicting one-phase properties for ethylene, especially for the density. It is perhaps not surprising that methane should be a better model than argon for the isotropic part of the potential for ethylene, and this is borne out by the results.

Literature Cited

(1) Angus, S., Armstrong, B., deReuck, K. M., Eds. "International Thermodynamic Tables of the Fluid State, Ethylene, 1972"; Butterworths: London, 1974.
(2) Douslin, D. R.; Harrison, R. H. *J. Chem. Thermodyn.* **1976**, *8*, 301.
(3) Hastings, J. R.; Levelt Sengers, J. M. H.; Balfour, F. W. *J. Chem. Thermodyn.* **1980**, *12*, 1009.
(4) Bender, E. *Cryogenics* **1975**, *15*, 667.
(5) Straty, C. G. *J. Chem. Thermodyn.* **1980**, *8*, 709.
(6) McCarty, R. D.; Jacobsen, R. T. *NBS Tech. Note (U.S)* **1981**, 1045.
(7) Gubbins, K. E.; Twu, C. H. *Chem. Eng. Sci.* **1978**, *33*, 863, 879.
(8) Gubbins, K. E.; Gray, C. G.; Machado, J. R. S. *Mol. Phys.* **1981**, *42*, 817.
(9) Streett, W. B.; Staveley, L. A. K. "Advances in Cryogenic Engineering"; Timmerhaus, K. D., Ed.; Plenum Press: New York, 1968; Vol. 13, p 363.
(10) Streett, W. B.; Staveley, L. A. K. *J. Chem. Phys.* **1971**, *55*, 2495.
(11) Streett, W. B.; Sagan, L. S.; Staveley, L. A. K. *J. Chem. Thermodyn.* **1973**, *5*, 633.
(12) Haynes, W. M. *Cryogenics* **1978**, *18*, 621.
(13) Menes, F.; Dorfmuller, T.; Bigeleisen, J. *J. Chem. Phys.* **1970**, *53*, 2869.
(14) Hust, J. G.; McCarty, R. D. *Cryogenics* **1967**, *7*, 200.
(15) McGlashan, M. L.; Potter, D. J. B. *Proc. R. Soc. London, Ser. A* **1962**, *267*, 478.
(16) McGlashan, M. L.; Wormald, C. J. *Trans. Faraday Soc.* **1964**, *60*, 646.
(17) Michels, A.; Geldermans, M. *Physica* **1942**, *9*, 967.
(18) Chueh, P. L.; Prausnitz, J. M. *AIChE J.* **1967**, *13*, 896.
(19) Clusius, K.; Konnertz, F. *Z. Naturforsch. A* **1949**, *4*, 117.
(20) Pople, J. A. *Proc. R. Soc. London, Ser. A* **1954**, *221*, 998.
(21) Gray, C. G.; Gubbins, K. E.; Twu, C. H. *J. Chem. Phys.* **1978**, *69*, 182.
(22) Stell, G.; Rasaiah, J. C.; Narang, H. *Mol. Phys.* **1974**, *23*, 393.
(23) Clancy, P.; Gubbins, K. E.; Gray, C. G. *Discuss. Faraday Soc.* **1976**, *66*, 116.
(24) Machado, J. R. S. M.S. Thesis, Cornell University, Ithaca, NY, 1979.
(25) Clancy, P.; Gubbins, K. E. *Mol. Phys.* **1981**, *44*, 581.
(26) Gosman, A. L.; McCarty, R. D.; Hust, J. D. *Natl. Stand. Ref. Data Ser. (U.S., Natl. Bur. Stand.)* **1969**, *27*.
(27) Twu, C. H.; Gubbins, K. E.; Gray, C. G. *J. Chem. Phys.* **1976**, *64*, 5186.
(28) Hostika, C.; Bose, T. K.; Sochanski, J. S. *J. Chem. Phys.* **1974**, *61*, 2575.
(29) Hills, G. W.; Jones, W. J. *J. Chem. Soc., Faraday Trans. 2* **1975**, *71*, 812.
(30) Angus, S.; Armstrong, B.; de Reuck, K. M. "International Thermodynamic Tables of Fluid State—5, Methane"; Pergamon Press: Oxford, 1977.
(31) Dagg, I. R.; Read, L. A. A.; Andrews, B. *Can. J. Phys.* **1981**, *59*, 57.

Received for review December 14, 1981. Accepted June 1, 1982. Acknowledgment is made to the donors of the Petroleum Research Fund, administered by the American Chemical Society, for partial support of this work. Additional support was provided under contract DE-AC02-79ER10422 A001 from the Division of Chemical Sciences of the Department of Energy. A.H. acknowledges a fellowship from the Deutsche Forschungsgemeinschaft.

Solubility of Cobalt Anthranilate in Water at Various Temperatures

Ishwari P. Saraswat

Chemistry Department, University of Roorkee, Roorkee 247 672, India

Sushil K. Suri*

Chemistry Department, Indian Institute of Technology, New Delhi 110 016, India

The solubility of cobalt anthranilate in water has been determined at 5 K intervals over the temperature range 273-328 K by using radioactive cobalt-57 as a tracer. The solubility results are indicative of a phase change in solid cobalt anthranilate at ~288 K.

* Address correspondence to this author at his present address: Hindustan Lever Research Centre, Andheri (East), Bombay 400 099, India.

Introduction

A large number of bivalent metal ions including Co^{2+} can be precipitated quantitatively by anthranilic acid (*1-4*). In the literature, the solubility product, K_s, of cobalt anthranilate (CA) in water has been reported at 298.15 K by two different schools (*2*, *5*). Yatsimirskii and Kharitonov (*2*) estimated $K_s = 1.2 \times 10^{-12}$ from the solubilities of CA in aqueous ammonia and acetate buffers. Lumme (*5*) reported $_pK_s = 0.90$ (which corresponds to $K_s = 0.13$) from potentiometric studies. Since the

0021-9568/82/1727-0385$01.25/0